Single-valley high-mobility (110) AlAs quantum wells with anisotropic mass

S. Dasgupta,[1,a)] S. Birner,[1] C. Knaak,[1] M. Bichler,[1] A. Fontcuberta i Morral,[1] G. Abstreiter,[1] and M. Grayson[2,b)]
[1]*Walter Schottky Institut, Technische Universität München, Garching D-85748, Germany*
[2]*Department of Electrical Engineering and Computer Science, Northwestern University, Evanston, Illinois 60208, USA and Walter Schottky Institut, Technische Universität München, Garching D-85748, Germany*

(Received 23 July 2008; accepted 9 September 2008; published online 29 September 2008)

We studied a doping series of (110)-oriented AlAs quantum wells (QWs) and observed transport evidence of single anisotropic-mass valley occupancy for the electrons in a 150 Å wide QW. Our calculations of strain and quantum confinement for these samples predict single anisotropic-mass valley occupancy for well widths W greater than 53 Å. Below this, double-valley occupation is predicted such that the longitudinal mass axes are collinear. We observed mobility anisotropy in the electronic transport along the crystallographic directions in the ratio of 2.8, attributed to the mass anisotropy as well as anisotropic scattering of the electrons in the X-valley of AlAs. © *2008 American Institute of Physics*. [DOI: 10.1063/1.2991448]

Strain and quantum confinement play an important role in tuning the valley degeneracy in indirect bandgap semiconductors.[1,2] Two dimensional electron systems[3,4] as well as one dimensional (1D)[5–7] systems in AlAs have been previously studied and analyzed for (001)-oriented quantum wells (QWs), both of which have a reduced valley degeneracy from the bulk. The 2D wide QWs have isotropic mobility resulting from doubly degenerate valleys with orthogonally oriented anisotropic masses. However, the other facets of growth, such as (110), have not been extensively explored. The knowledge of the doping efficiency for this orientation is necessary to grow optimally doped cleaved-edge overgrown quantum wires[5,6] and the valley degeneracy is expected to be different from (001) oriented wells. In this paper, we present an experimental study of a doping series of double-sided-doped QWs grown in (110)-orientation and show experimental evidence of single-valley occupancy and anisotropic electron mass for these QWs. This has been further complemented with effective mass calculations with finite barrier that take strain into account, which explain how for (110)-oriented AlAs QWs, single-valley occupation is expected for the square well width $W>53$ Å. Also, we deduced donor binding energy and doping efficiency. Previously, anisotropic single-valley systems have only been investigated in piezostrained (001) AlAs samples.[8,9] In contrast, the (110) AlAs samples investigated in this letter are singly degenerate as a result of the growth orientation, require no additional piezo sample preparation to reach single-valley occupancy, and tend to show comparable mobilities to those reported in piezostrained samples.

Bulk AlAs is an indirect band gap III-V semiconductor with three degenerate conduction band valleys at the X-points of the Brillouin zone edge. The mass of each valley is anisotropic, with heavy longitudinal and light transverse mass $m_l=1.1m_e$ and $m_t=0.2m_e$, respectively.[3,10,11] In a 2D-confined system, the number of degenerate X-points depends on the growth direction and the QW width W due to a balance of strain and confinement effects. For (001)-oriented QWs studied elsewhere with $W<55$ Å, a single X-valley is occupied whereas $W>55$ Å yields doubly degenerate occupied X-valleys in the QW.[12]

We determine in this work how (110) QW valley degeneracy should depend on well width. The energy $E_\tau(\mathbf{k})$ of an electron in a valley X_τ with index τ $(=x,y$ or $z)$ is

$$E_\tau(\mathbf{k}) = E_{\mathrm{kin}}(\mathbf{k}) + E_{0,\tau} + \Delta_\tau(\mathbf{k}), \tag{1}$$

where E_{kin} is the in-plane kinetic energy, $\mathbf{k}$ is the 2D in-plane momentum relative to the τ-valley minimum, $E_{0,\tau}$ is the ground confinement energy, and Δ_τ is the strain induced energy shift at the Brillouin zone edge at the X-point.

It is useful to introduce the cubic crystal axes $\vec{\mathbf{x}}=(x,y,z)$ and the growth axes $\vec{\mathbf{a}}=(a,b,z)=\mathbf{R}\vec{x}$,[5] related by the rotational transformation (Fig. 1)

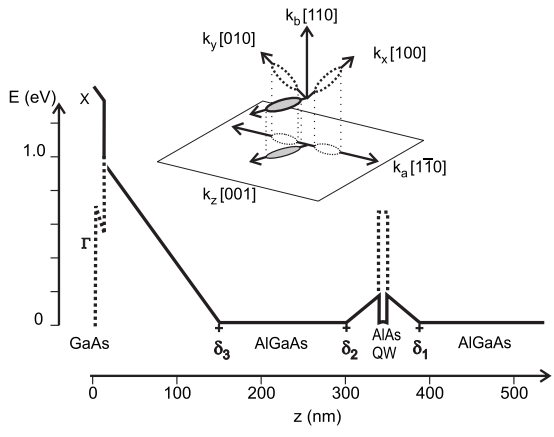

FIG. 1. Energy band structure of the triple delta-doped (110) AlAs QW. The vertical axis denotes the energy scale, the+denotes the Si-delta doping layers in the AlGaAs layers, the solid line shows the X band, and the dashed line shows the Γ band. The structure is the same as described in Ref. 4 on a different facet. (Inset) Electron occupation in a (110)-oriented QW, in momentum space. The b-axis denotes the growth axis, and the single-valley case is shown as shaded ellipsoid (double-valley unshaded).

a)Electronic mail: dasgupta@wsi.tum.de.
b)Author to whom correspondence should be addressed. Electronic mail: m-grayson@northwestern.edu.

$$\mathbf{R} = \begin{bmatrix} 1/\sqrt{2} & -1/\sqrt{2} & 0 \\ 1/\sqrt{2} & 1/\sqrt{2} & 0 \\ 0 & 0 & 1 \end{bmatrix}. \quad (2)$$

Confinement energies are best determined by transforming the mass tensor to the growth-basis $\vec{\mathbf{a}}$. In the crystal-basis $\vec{\mathbf{x}}$, the mass tensor $(\mathbf{m}_{ij}^{\tau})^{-1}$ for the τth valley is diagonal with $\mathbf{m}_{\tau\tau}^{\tau}=m_{\mathrm{l}}$ and $\mathbf{m}_{ii}^{\tau}=m_{\mathrm{t}}$ for $i\neq\tau$. Transforming to the growth-basis $\vec{\mathbf{a}}$, the mass tensor becomes $(\bar{\mathbf{m}}^{\tau})^{-1}=\mathbf{R}(\mathbf{m}^{\tau})^{-1}\mathbf{R}^{-1}$, so for the X_x-valley, for example, with $\tau=x$

$$(\mathbf{m}^{x})^{-1} = \begin{bmatrix} 1/m_d & 1/m_f & 0 \\ 1/m_f & 1/m_d & 0 \\ 0 & 0 & 1/m_t \end{bmatrix}, \quad (3)$$

with diagonal $m_d=2m_lm_t/(m_l+m_t)$ and off-diagonal $m_f=2m_lm_t/(m_t-m_l)$ mass terms. The diagonal mass enters the Schrödinger equation for the QW confinement energy.

Deformation potential energies are best determined by transforming the strain tensor to the crystal-basis $\vec{\mathbf{x}}$. We assume that the AlAs QW ($a_{\mathrm{AlAs}}=5.65252$ Å) is strained relative to the GaAs substrate lattice ($a_{\mathrm{GaAs}}=5.64177$ Å) in agreement with previous publications.[13–15] For (110) biaxial strain, the perpendicular component can be deduced from the in-plane strain as $\varepsilon_{\perp}=-D\cdot\varepsilon_{\parallel}$, where $D=0.6165$ is a constant that depends on the interface orientation and on the elastic constants of AlAs.[13,16] In the growth-basis $\vec{\mathbf{a}}$, $(0,b,0)$ is the growth direction, and the strain tensor $\bar{\varepsilon}_{ij}$ is diagonal with $\bar{\varepsilon}_{aa}=\bar{\varepsilon}_{zz}=\varepsilon_{\parallel}$, and $\bar{\varepsilon}_{bb}=\varepsilon_{\perp}$. Transforming to the $\vec{\mathbf{x}}$-basis, the strain tensor becomes $\varepsilon=\mathbf{R}^{-1}\bar{\varepsilon}\mathbf{R}$ with diagonal terms $\varepsilon_{xx}=\varepsilon_{yy}=\varepsilon_{\perp}+\varepsilon_{\parallel}/2$ and $\varepsilon_{zz}=\varepsilon_{\parallel}$.[13,16] The energy at the τ^{th} valley minimum shifts from the unstrained case by an amount $\Delta^{\tau}=\Xi\varepsilon_{\tau\tau}$, where $\varepsilon_{\tau\tau}$ is defined in the crystal-basis $\vec{\mathbf{x}}$, and the deformation potential for AlAs is $\Xi=6.11$ eV.[13] In our case, the single and double-degenerate X band edges are separated by 9 meV. Combining these band edges with knowledge of the mass tensor, the Schrödinger equation can now be solved. All this information is automatically included in the publicly available simulation software NEXTNANO^3 (Ref. 17) yielding a cross-over width $W_c=53$ Å.

For $W>W_c$, there is only a single occupied in-plane valley shown in shaded gray in the inset of Fig. 1. The two higher-energy out-of-plane valleys are shown as dotted ellipsoids. For $W<W_c$ the role reverses, and these out-of-plane valleys become occupied. The projection of these valleys would be the white ellipsoids in the plane of the QW. Hence, the two valleys would have collinear longitudinal mass axes, in contrast to the (001) QW case where they are orthogonal.

Samples were grown on (110) GaAs substrates using molecular beam epitaxy. The structure of the samples is similar to Ref. 4 for the (001) facet (Fig. 1). There is a 150 Å wide QW with three Si δ-doping layers. δ_1 and δ_2 separated from the QW by $\mathrm{Al}_{0.45}\mathrm{Ga}_{0.55}\mathrm{As}$ spacers provide electrons to the QW. These two δ-doping layers are doped equally with a Si density $n_{\delta_1}=n_{\delta_2}=n_{\mathrm{Si}}$. The Si doping near the surface has higher density $n_{\delta_3}=2.7n_{\mathrm{Si}}$ and satisfies the surface states to pin the conduction band to the donor binding energy upon saturation. Various samples were grown with different doping n_{Si} indexed G through M.[18]

Indium contacts were annealed at 450 °C for 100 s. Two-point contact resistance was around 100 kΩ at 300 K and around 40 kΩ at 4.2 K. Samples were illuminated using a red light emitting diode (LED) of wavelength 635 nm. We performed postillumination annealing (PIA) at around 25 K for these samples, described previously for (001) AlAs samples,[4] to obtain persistent photoconductivity. Typical longitudinal (R_{xx}) and transverse (R_{xy}) resistance variation with magnetic field at 330 mK in the dark and postillumination for sample J in van der Pauw geometry is plotted in Fig. 2. The density of the samples in subsequent figures were deduced from such measurements.

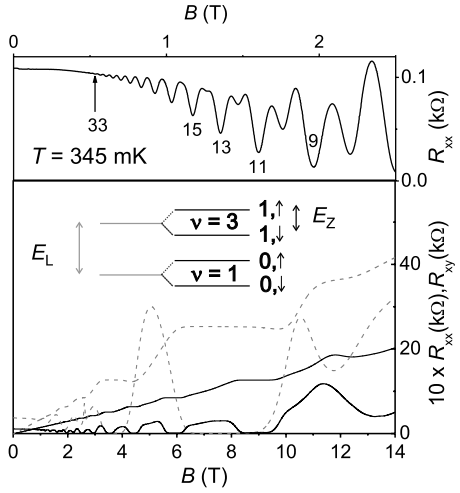

FIG. 2. (Bottom) R_{xx} and R_{xy} traces at 345 mK in the dark (dashed) and postillumination (solid) for sample J in van der Pauw configuration. In the dark, $n=1.8\times10^{11}$ cm^{-2} and $\mu=0.40\times10^5$ cm^2/V s and postillumination, $n=3.5\times10^{11}$cm^{-2} and $\mu=0.53\times10^5$ cm^2/V s. (Top) Postillumination longitudinal resistance for sample L at low magnetic fields. Odd periodicity, of prominent minima, is one indication of single-valley occupancy. Ladder diagram inset shows Landau level splitting E_L and Zeeman splitting E_Z for bare $g^*m^*\sim1$. The prominence of odd integer gaps suggests $g^*m^*>1$ with interactions.

The first evidence of single-valley occupancy for (110) orientation comes from the $\nu=2n+1$ periodicity at low magnetic field Shubnikov–de Haas oscillations for the PIA data (Fig. 2, top). Due to the heavy cyclotron mass in AlAs, $m^*=(m_lm_l)^{1/2}=0.47m_e$ and large Lande g-factor of $g^*=2$,[19] the bare Zeeman energy E_Z is about half the bare cyclotron energy E_L, so that $m^*g^*\sim1$ in the absence of interactions, the case shown in the inset of Fig. 2. Exchange and correlation enhancement of $m^*g^*\sim1$ is known to occur in AlAs quantum Hall systems,[9] and for the range $1<m^*g^*<2$, the Zeeman gap will be larger than the cyclotron gap and odd filling factor $\nu=2n+1$ will dominate at low fields. As shown in the data of Fig. 2 (top), the odd integers clearly dominate $\nu=9$ upward and persist to filling factors as high as $\nu=33$. In double-valley systems, by comparison, an additional factor of 2 appears in the filling factor due to valley degeneracy, and one observes prominent gaps in the series $\nu=4n+2$.[4]

The second evidence of single-valley occupancy comes from the anisotropic mobility in (110) QWs. We performed mobility measurements on a L-shaped Hall bar fabricated along the crystallographic axes [001] and [1$\bar{1}$0]. The densities in both arms are found to be the same, $n=1.65\times10^{11}$ cm^{-2}/V, and the mobilities in the two directions are $\mu_{[001]}=0.3\times10^5$ cm^2/V s and $\mu_{[1\bar{1}0]}=1.0\times10^5$ cm^2/V s. The mobility anisotropy is consistent with anisotropic mass electrons conducting in a single valley with the heavy mass oriented along the [001] direction and the light mass along

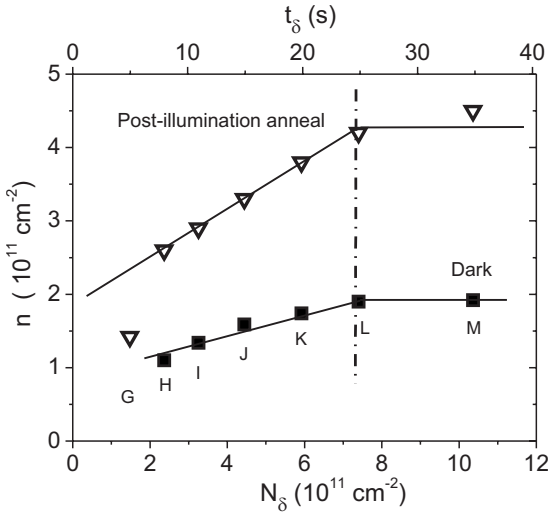

FIG. 3. The density of 2DES in a (110)-oriented AlAs QW as a function of the Si δ-doping n_{Si}. The top x-axis defines the time of Si doping corresponding to the doping densities. The vertical dashed line shows the saturation threshold n_{sat} for both the dark and the postillumination (red LED ∇) conditions. The solid lines are plotted as an aid to locating the saturation threshold.

the $[1\bar{1}0]$ direction, as expected in the single-valley degenerate system. We note that a naive Drude model of mobility is not sufficient since the mobility ratio is $\mu_{[1\bar{1}0]}/\mu_{[001]}=2.8$, whereas the inverse mass ratio is $m_{[001]}/m_{[1\bar{1}0]}=m_l/m_t=5.5$. There have been previous publications reporting similar non-Drude effects in anisotropic mass systems,[19] and like these authors we propose that anisotropic scattering is responsible.[20]

When the mobility is measured using van der Pauw geometry, one obtains the mobility,[21] $\mu_{\mathrm{vdP}}=0.40\times10^5\ \mathrm{cm}^2/\mathrm{V\,s}$. This can be related to the mobility in each crystallographic direction $\mu'_{\mathrm{vdP}}=(\mu_{xx}\mu_{yy})^{1/2}$.[22] For our sample, $\mu'_{\mathrm{vdP}}=0.50\times10^5\ \mathrm{cm}^2/\mathrm{V\,s}$, within reasonable agreement to the van der Pauw mobility.

In Fig. 3, the 2DES density of the samples are plotted as a function of different Si doping concentrations n_{Si} deduced from the doping times t_{Si} with a calibrated Si flux of $2.9\times10^{10}\ \mathrm{cm}^{-2}\ \mathrm{s}^{-1}$ for 11.4 A heater current. The dark electron density is seen to saturate at around $n_{\mathrm{DK}}=1.9\times10^{11}\ \mathrm{cm}^{-2}$. PIA density, plotted as triangles, is seen to saturate at about $n_{\mathrm{PIA}}=4.2\times10^{11}\mathrm{cm}^{-2}$. Sample L represents the optimally doped sample, since at higher doping approximiately the same saturation density n_{PIA} is observed. Sample G works only postillumination. In the lowest density sample G, the postillumination density drops abruptly, most likely indicating that the surface δ-doping layer is no longer in saturation. From the experimental dark density of n_{DK}, we deduce a donor binding energy of $\Delta_{\mathrm{DK}}=66$ meV and for n_{PIA}, we deduce the postillumination saturation binding energy of $\Delta_{\mathrm{PIA}}=0$ meV using the same analysis presented in a previous publication.[4] The doping efficiency for the samples in the dark and postillumination was calculated using the doping density n_{Si} at the saturation threshold shown with a vertical dashed line. We define from Ref. 4,

$$\eta_{\mathrm{DK,PIA}}=\frac{n_{\mathrm{DK,PIA}}}{2n_{\mathrm{Si}}}, \tag{4}$$

where η is the doping efficiency. The factor of 2 in the denominator arises from the double-sided δ-doping layers, assuming that all surface states have been screened by the top δ-layer. Using this equation, we obtain the doping efficiency of $\eta_{\mathrm{DK}}=7\%$ in the dark and $\eta_{\mathrm{PIA}}=15\%$ PIA.

In summary, we have shown experimentally the occupation of the single X-valley by the 2DES in AlAs QWs in this (110) orientation, which shows anisotropic mobility that can be partly attributed to the mass anisotropy. We have also presented results of a model calculation for the cross-over width in AlAs for (110) orientation, which defines the QW width below which double valleys are occupied and above which a single valley is occupied. Furthermore, we have determined the binding energy of Si in δ-doped layers in $Al_{0.45}Ga_{0.55}As$ in the dark and after illumination for the (110) orientation and found them to be in the range of the values found for (001) orientation. The doping efficiency for the Si δ-layers has been calculated to be 7% in the dark and 15% PIA. These parameters will be instrumental in optimizing mobility in (110)-oriented AlAs QWs and cleaved-edge overgrowth structures.

This work was funded by BMBF nanoQUIT Project No. 01BM470 and the Nanosystems Initiative Munich (NIM).

[1] Y. Sun, S. E. Thompson, and T. Nishida, J. Appl. Phys. **101**, 104503 (2007).
[2] S. Dhar, E. Ungersböck, H. Kosina, T. Grasser, and S. Selberherr, IEEE Trans. Nanotechnol. **6**, 97 (2007).
[3] M. Shayegan, E. P. De Poortere, O. Gunawan, Y. P. Shkolnikov, E. Tutuc, and Phys. Status Solidi B **243**, 3629 (2006).
[4] S. Dasgupta, C. Knaak, J. Moser, M. Bichler, S. F. Roth, A. Fontcuberta i Morral, G. Abstreiter, and M. Grayson, Appl. Phys. Lett. **91**, 142120 (2007).
[5] J. Moser, T. Zibold, D. Schuh, M. Bichler, F. Ertl, G. Abstreiter, M. Grayson, and S. Roddaro, Appl. Phys. Lett. **87**, 052101 (2005).
[6] J. Moser, S. Roddaro, D. Schuh, M. Bichler, V. Pellegrini, and M. Grayson, Phys. Rev. B **74**, 193307 (2006).
[7] O. Gunawan, B. Habib, E. P. De Poortere, and M. Shayegan, Phys. Rev. B **74**, 155436 (2006).
[8] K. Vakili, Y. P. Shkolnikov, E. Tutuc, N. C. Bishop, E. P. De Poortere, and M. Shayegan, Physica E (Amsterdam) **34**, 89 (2006).
[9] M. Padmanabhan, T. Gokmen, N. C. Bishop, and M. Shayegan, Phys. Rev. Lett. **101**, 026402 (2008).
[10] O. Gunawan, Y. P. Shkolnikov, E. P. De Poortere, E. Tutuc, and M. Shayegan, Phys. Rev. Lett. **93**, 246603 (2004).
[11] O. Gunawan, E. P. De Poortere, and M. Shayegan, Phys. Rev. B **75**, 081304 (2007).
[12] A. F. W. van de Stadt, P. M. Koenraad, J. A. A. J. Perenboom, and J. H. Wolter, Surf. Sci. **361**, 521 (1996).
[13] C. G. Van de Walle, Phys. Rev. B **39**, 1871 (1989).
[14] J. A. Carlin, S. A. Ringel, R. N. Sacks, and K. S. Yap, J. Vac. Sci. Technol. B **16**, 1372 (1998).
[15] H. W. van Kesteren, E. C. Cosman, P. Dawson, K. J. Moore, and C. T. Foxon, Phys. Rev. B **39**, 13426 (1989).
[16] M. P. C. M. Krijn, Semicond. Sci. Technol. **6**, 27 (1991).
[17] www.nextnano.de; the tutorial for the 1D AlAs QW cross-over width W_c is publicly available for (001)- and (110)-oriented AlAs QWs. Simulations for the (001) facet under the same assumptions give $W_c=54$ Å, in excellent agreement with the experimentally observed cross-over of 55 Å.
[18] G:06-15-07.2; H:06-15-07.1; I:05-08-07.1; J:05-08-07.2; K:01-30-07.1; L:01-05-07.2; M:01-30-07.2.
[19] D. Bishop, R. C. Dynes, B. J. Lin, and D. C. Tsui, Phys. Rev. B **30**, 3539 (1984).
[20] Y. Tokura, Phys. Rev. B **58**, 7151 (1998).
[21] L. J. van der Pauw, Philips Res. Rep. **13**, 1 (1958).
[22] L. J. van der Pauw, Philips Res. Rep. **16**, 187 (1961).